Chemical Science

ROYAL SOCIETY OF CHEMISTRY

EDGE ARTICLE

View Article Online
View Journal | View Issue

Cite this: *Chem. Sci.*, 2024, **15**, 10126

All publication charges for this article have been paid for by the Royal Society of Chemistry

Received 22nd March 2024
Accepted 23rd May 2024

DOI: 10.1039/d4sc01918k

rsc.li/chemical-science

Generic and facile mechanochemical access to versatile lattice-confined Pd(II)-based heterometallic sites†

Zhuorigebatu Tegudeer,[a] Jisue Moon,[b] Joshua Wright,[c] Milton Das,[d] Gayan Rubasinghege,[d] Wenqian Xu[e] and Wen-Yang Gao *[a]

Metal–organic frameworks (MOFs) show remarkable potential in a broad array of applications given their physical and chemical versatility. Classical synthesis of MOFs is performed using solution chemistry at elevated temperatures to achieve reversible metal–ligand bond formation. These harsh conditions may not be suitable for chemical species sensitive to high temperature or prone to deleterious reactions with solvents. For instance, Pd(II) is susceptible to reduction under solvothermal conditions and is not a common metal node of MOFs. We report a generic and facile mechanochemical strategy that directly incorporates a series of Pd(II)-based heterobimetallic clusters into MOFs as metal nodes without Pd(II) being reduced to Pd(0). Mechanochemistry features advantages of short reaction time, minimum solvent, high reaction yield, and high degree of synthetic control. Catalytic performances of lattice-confined heterobimetallic sites are examined for nitrene transfer reactions and we demonstrate that the chemoselectivity for allylic amination *versus* olefin aziridination is readily tuned by the identity of the first-row metal ion in Pd(II)-based heterobimetallic clusters.

Introduction

Metal–organic frameworks (MOFs)[1,2] have garnered escalating attention as a type of crystalline porous materials and demonstrated their promising applications in gas storage,[3,4] separation,[5–7] catalysis,[8–11] and others.[12,13] Their crystallinity is usually achieved by reversible metal–ligand (M–L) bond formation reactions carried out under solvo(hydro)thermal conditions, which allows structures to be determined by X-ray diffraction experiments. However, such harsh reaction conditions may impose a synthetic challenge to build MOFs based on chemical species that typically involve side reactions in the solution at high temperature. For example, while Pd catalysts realize a variety of meaningful reactions in organic transformations,[14–16] palladium(II) can be easily reduced into Pd(0) *via* β-hydride elimination, which aggregates to form Pd black.[17,18] Given attractive and unique binding and catalytic properties of Pd(II) sites, especially being solidified in accessible pore space, Pd(II)-containing MOFs have become highly appealing and desirable synthetic targets with very limited examples since the beginning of the MOF era.[19–21] Compared to the abundance of MOFs based on other transition metals, especially the first-row transition ones, the number of Pd(II)-based MOFs is rather scarce partially due to this synthetic barrier.[20,22,23] While postsynthetic metal metathesis has been employed to obtain Pd(II)-containing MOFs (Fig. 1a),[24–26] it requires a lengthy reaction time and still lacks control over the metal composition and distribution in the resultant materials. Meanwhile, two inspiring case studies that employ Pd(II)-based paddlewheel heterobimetallic molecular complexes, $PdM(OAc)_4$, as precursors to build MOFs (M = Cu)[27] and discrete metal–organic polyhedra (M = Cu, Zn, or Ni),[28] have been known to introduce Pd(II) sites into MOFs using solution chemistry. It is worth noting that only ambient room temperature was pursued in both cases, which is hypothesized to avoid possible reduction of Pd(II).[29] Thus, a generic synthetic strategy to incorporate Pd(II) into a broad family of MOF lattices is still profoundly motivating.

In contrast to the mainstream conventional solvothermal method, solid-state mechanochemistry is emerging into a distinctive and facile alternative to access crystalline MOFs, which exhibits sustainable synthetic advantages with regard to

[a]*Department of Chemistry and Biochemistry, Ohio University, Athens, Ohio 45701, USA. E-mail: gaow@ohio.edu*

[b]*Chemical Sciences Division, Oak Ridge National Laboratory, Oak Ridge, Tennessee 37831, USA*

[c]*Department of Physics, Illinois Institute of Technology, Chicago, Illinois 60616, USA*

[d]*Department of Chemistry, New Mexico Institute of Mining and Technology, Socorro, New Mexico 87801, USA*

[e]*X-ray Science Division, Advanced Photon Source, Argonne National Laboratory, Lemont, Illinois 60439, USA*

† Electronic supplementary information (ESI) available: Details of synthesis and characterization using powder X-ray diffraction, X-ray absorption, infrared spectroscopy, UV-vis diffuse reflectance spectroscopy, inductively coupled plasma mass spectrometry, N_2 adsorption isotherms, thermogravimetric analysis, and others. See DOI: https://doi.org/10.1039/d4sc01918k

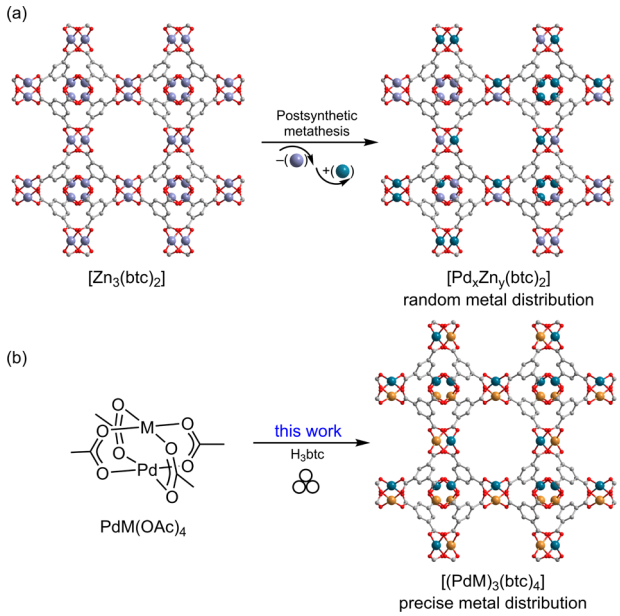

Fig. 1 (a) The developed postsynthetic metal metathesis approach lacks control over the metal composition and distribution in the resultant MOFs. (b) This work introduces mechanochemistry as an effective synthetic strategy to build a series of Pd(II)-derived MOFs with precise metal composition and distribution.

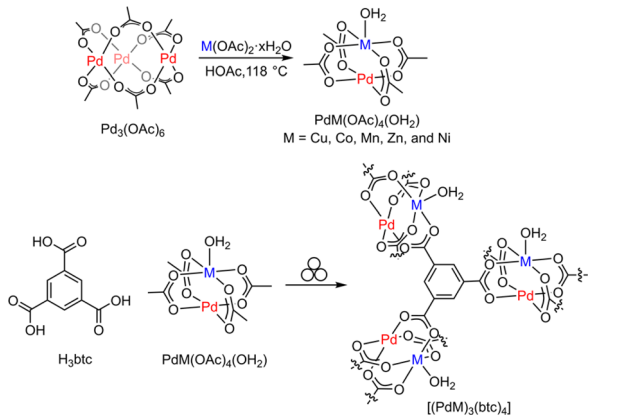

Fig. 2 A family of paddlewheel heterobimetallic molecular complexes are readily available by refluxing $Pd(OAc)_2$ and $M(OAc)_2 \cdot xH_2O$ (M = Cu, Co, Mn, Zn, and Ni) in acetic acid. These molecular complexes serve as critical precursors for the formation of Pd(II)-derived heterobimetallic MOFs under mechanochemical reaction conditions.

the solvent volume reduction, short reaction time, and high yield.[30–40] Following the pioneering work done by James *et al.*,[41] exciting progress has been continuously made in the field of mechanochemical synthesis of MOFs by James,[41–44] Friščić,[45–48] Užarević,[49–51] Emmerling,[52–56] Lewiński,[57–59] Holman,[60–63] Li[64–66] and others,[67–73] For instance, pre-installed cluster precursors often dictate the geometry of metal nodes in the resultant MOFs.[74,75] Milling reactivity or outcome can be influenced by the liquid additive or drying agent in the reaction mixture.[76,77] The reticular chemistry principle remains applicable to mechanochemical synthesis offering pore size control of MOFs.[78,79] More importantly, it presents a valuable opportunity to introduce chemical species that are not compatible with solvothermal conditions into MOF lattices, while the mild mechanochemical conditions eliminate potential pathways of side reactions for those sensitive motifs. Herein we report our systematic work that leverages the facile mechanochemical synthesis to readily build a family of versatile Pd(II)-based heterobimetallic porous MOFs (Fig. 1b) based on heterobimetallic tetraacetate paddlewheel molecular complexes, $PdM(OAc)_4$ (M = Cu, Zn, Mn, Co, and Ni), without Pd(II) being reduced to Pd(0).

Results and discussion

We initiated these investigations by preparing a series of paddlewheel heterobimetallic molecular complexes, $PdM(OAc)_4$ (M = Cu, Zn, Co, Mn, and Ni) by refluxing $Pd(OAc)_2$ and $M(OAc)_2 \cdot xH_2O$ in acetic acid (Fig. 2).[80] These crystalline complexes were harvested and examined by powder X-ray diffraction (PXRD, Fig. S1–S5†), solution UV-vis spectroscopy (Fig. S6†), and infrared (IR, Fig. S7†) spectroscopy, and the results are consistent with the reported data.[80] Then we explored mechanochemical synthesis to access a porous crystalline material of $[(PdCu)_3(btc)_4]$ by ball-milling $PdCu(OAc)_4$ and 1,3,5-benzenetricarboxylic acid (H_3btc) in a 3 : 4 stoichiometric molar ratio (Fig. 2). Milling a mixture of $PdCu(OAc)_4$ and H_3btc in the presence of ethanol (EtOH, $\eta = 0.60$ μL mg^{-1}) for 0.75 h afforded a dark green colored crystalline solid that we assign as $[(PdCu)_3(btc)_4]$. PXRD analysis indicates that the obtained material is isostructural to the classic $[Cu_3(btc)_2]$ or HKUST-1 (Fig. 3a and S8†).[52,81,82] For comparison, milling a 3 : 2 mixture of $Pd(OAc)_2$ and H_3btc under similar reaction conditions did not afford $[Pd_3(btc)_2]$ and only generated amorphous solids (Fig. S9†). This is probably attributed to palladium(II) acetate displaying a thermodynamically preferred acetate-bridged trimer (Fig. 2),[83,84] instead of the paddlewheel dimer. Thus, the preformed paddlewheel molecular geometry of $PdCu(OAc)_4$, similar to $Cu_2(OAc)_4$, appears to be critical for the successful mechanochemical synthesis. Additionally, the presence of EtOH as the assisting liquid during the mechanochemistry is also crucial, which is highlighted since milling a 3 : 4 mixture of $PdCu(OAc)_4$ and H_3btc under neat conditions (without any liquid) did not produce any crystalline phase of $[(PdCu)_3(btc)_4]$ (Fig. S9†). The effect of liquid additive on milling formation of $[Cu_3(btc)_2]$ was discussed in great detail previously.[76]

X-ray absorption near-edge structure (XANES) data for the Pd (Fig. 4a) and Cu (ESI, Fig. S10†) K-edge suggest that the oxidation states of Pd(II) and Cu(II) were observed in $[(PdCu)_3(btc)_4]$ without the presence of Pd(0), similar to that of $Pd(OAc)_2$ and $Cu(OAc)_2 \cdot H_2O$. Furthermore, Pd and Cu K-edge extended X-ray absorption fine structure (EXAFS) data (Fig. 4b, S11 and S12†) collected for $[(PdCu)_3(btc)_4]$ indicate that the local coordination geometry of $PdCu(OOC)_4$ is unchanged under the mechanochemical conditions, similar to that of $PdCu(OAc)_4$. Specifically, the EXAFS data of $[(PdCu)_3(btc)_4]$ collected at the Pd K-edge (Fig. S11 and Table S1†) are consistent with the presence of a square-planar Pd(II) environment composed of two Pd–O

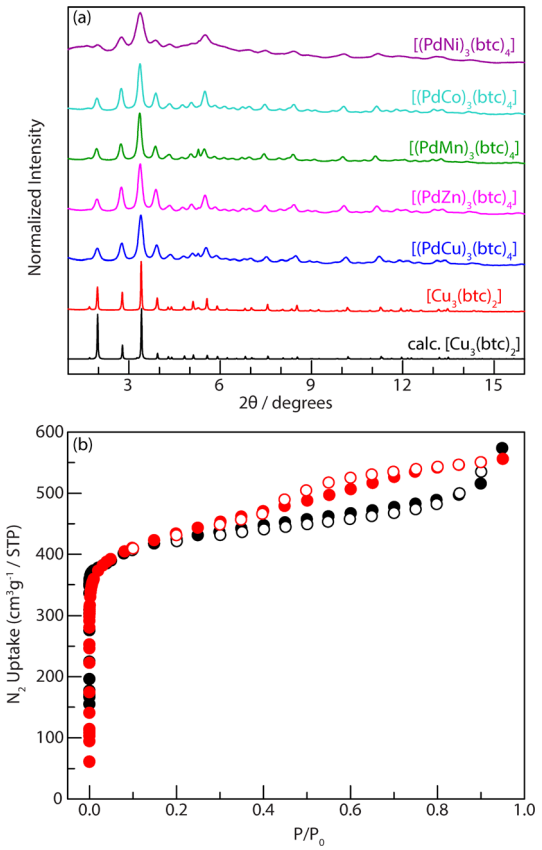

Fig. 3 (a) The mechanochemically obtained $[(PdM)_3(btc)_4]$ displays PXRD patterns (M = Cu, —; Zn, —; Mn, —; Co, —; Ni, —), which are consistent with the ones collected from the mechanochemically synthesized $[Cu_3(btc)_2]$ (—) and the calculated $[Cu_3(btc)_2]$ (—). The PXRD data were collected or calculated using $\lambda = 0.45212$ Å. (b) N_2 adsorption isotherms of the mechanochemically synthesized $[Cu_3(btc)_2]$ (adsorption (●), desorption (○)) and $[(PdCu)_3(btc)_4]$ (adsorption (●), desorption (○)) were measured at 77 K.

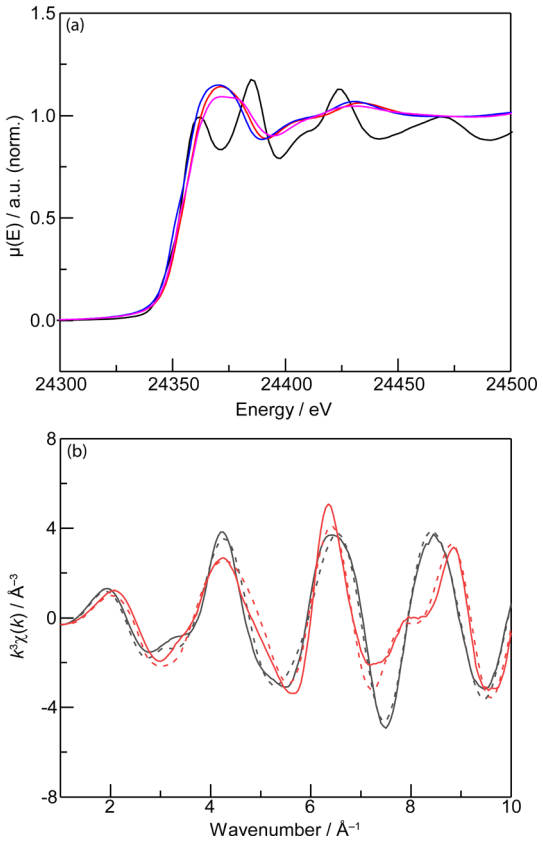

Fig. 4 (a) Pd K-edge XANES spectra of Pd(0) foil (—), $Pd(OAc)_2$ (—), and $PdCu(OAc)_4(OH_2)$ (—), and $[(PdCu)_3(btc)_4]$ (—).These spectra highlight that a common Pd(II) oxidation state is observed in $Pd(OAc)_2$, $PdCu(OAc)_4(OH_2)$, and $[(PdCu)_3(btc)_4]$, a significant departure from Pd(0) and the mechanochemical process does not generate Pd(0). (b) Pd K-edge EXAFS data (fitting range 1.0–10.0 $Å^{-1}$) in the *k*-space for $PdCu(OAc)_4(OH_2)$ (experimental data (—) and fit (- - - -)) and $[(PdCu)_3(btc)_4]$ (experimental data (—) and fit (----)).

distances at 1.90(1) Å and the other two at 2.36(1) Å along with one Pd–Cu distance at 2.83(1) Å, which is consistent with the molecular structure of $PdCu(OAc)_4$.[80] Meanwhile, analysis of the Cu K-edge EXAFS data (Fig. S12 and Table S2†) of $[(PdCu)_3(btc)_4]$ reveals the presence of an elongated octahedral Cu(II) environment composed of two equatorial Cu–O distances at 1.91(1) Å and two at 2.07(1) Å, and one axial Cu–O distance at 2.10(1) Å, which is also consistent with the molecular structure of $PdCu(OAc)_4$.

The reaction progress of mechanochemistry is monitored through IR spectroscopy by the disappearance of the carbonyl stretch at 1720 cm^{-1} and C–O stretch at 1273 cm^{-1} from free carboxylic acid groups (Fig. S13†).[85] Thermogravimetric analysis (TGA) of $[(PdCu)_3(btc)_4]$ indicated that this material is thermally stable up to 265 °C, which is comparable to the thermal stability of $[Cu_3(btc)_2]$ (Fig. S14†). Based on these observations, $[(PdCu)_3(btc)_4]$ was activated by exhaustive dichloromethane exchange followed by heating at 100 °C under vacuum prior to gas adsorption analysis. The permanent porosity of $[(PdCu)_3(btc)_4]$ was evaluated by N_2 adsorption isotherm analysis at 77 K (Fig. 3b). $[(PdCu)_3(btc)_4]$ has a measured Brunauer–Emmett–Teller (BET) surface area of 1517 $m^2\ g^{-1}$ (P/P_0 = 0.02–0.15), which is comparable to the measured BET surface area value (1518 $m^2\ g^{-1}$) of the mechanochemically prepared $[Cu_3(btc)_2]$. A known solution method at room temperature between $PdCu(OAc)_4$ and H_3btc affords $[(PdCu)_3(btc)_4]$ with a much lower surface area value at 1175 $m^2\ g^{-1}$.[40] The metal composition of $[(PdCu)_3(btc)_4]$ was investigated by inductively coupled plasma mass spectrometry (ICP-MS) of samples digested with hydrochloric acid or nitric acid (ESI, Table S3†). ICP-MS provided a Pd/Cu ratio of 1 : 1.06, which is consistent with the metal ratio in the molecular complex. The solid-state UV-vis diffuse reflectance spectrum of $[(PdCu)_3(btc)_4]$ bears a resemblance to that of $PdCu(OAc)_4$, but is much unlike that of $[Cu_3(btc)_2]$ (Fig. S15†). The electronic absorption features sustain from the molecular complex to the extended heterobimetallic lattice, which serves as additional evidence for the unchanged heterobimetallic electron configuration through the mechanochemistry.

The developed mechanochemical synthesis of $[(PdCu)_3(btc)_4]$ immediately provides access to other isostructural

extended MOF materials, $[(PdM)_3(btc)_4]$ (M = Zn, Mn, Co, and Ni, see details in ESI†), which are built upon their respective heterobimetallic molecular complexes. Their lattices, isostructural to $[Cu_3(btc)_2]$, were confirmed by PXRD (Fig. 3a). It is worth noting that the obtained $[(PdNi)_3(btc)_4]$ displays broader PXRD peaks than other heterobimetallic MOFs regardless of extensive attempts by varying milling time and the amount of additive EtOH. This is tentatively ascribed to the relatively slow ligand exchange kinetics of Ni(II),[86] leading to poor reversibility of M–L bond formation.[87] Other characterization data, including IR spectra (Fig. S16†), N_2 adsorption isotherms at 77 K (Fig. S17 and Table S4†), XANES and EXAFS data (Fig. S18–S27, Tables S5 and S6†), ICP-MS data (Table S3†), and UV-vis diffuse reflectance spectra (Fig. S28†), were collected on those mechanochemically generated heterobimetallic MOFs. More importantly, based on XANES data collected for all the molecular heterobimetallic complexes and their resultant MOFs, it is revealed that Pd(II) is maintained through the mechanochemical reactions as the only oxidation state observed across these samples in the absence of Pd(0) and first-row transition metals maintain the 2+ oxidation state after the mechanochemistry.

In addition to the advantages of ambient reaction temperature, minimum additive solvent, and short reaction time, the near solid-state reactions enable us to control the metal composition of multi-metallic MOFs by modulating the ratio of metal precursors at will.[50] For instance, a family of multimetallic MOF materials, isostructural to $[(PdCu)_3(btc)_4]$ or $[Cu_3(btc)_2]$, were immediately obtained by milling two, three, or four types of heterobimetallic molecular complexes together with H_3btc *via* the developed mechanochemistry. Their crystallinity is confirmed by PXRD (Fig. 5) and the metal ratios analyzed by ICP-MS (Table S7†) are consistent with the reaction stoichiometries.

Previously, only $PdCo(OAc)_4$ has been experimentally investigated as a potential catalyst for nitrene transfer chemistry using iminoiodinane reagents as nitrene sources.[88,89] Herein we have systematically examined catalytic performances of heterobimetallic molecular complexes, $PdM(OAc)_4$ (M = Cu, Zn, Mn, and Co), toward amination reaction of *trans*-4-hexenyl sulfamate (**1**) generating products of allylic amination (**2**) and olefin aziridination (**3**) (Table 1). In particular, $PdCo(OAc)_4$ proves to be the most efficient among various heterobimetallic molecular complexes with a total yield of 85% (entry 1, Table 1). Meanwhile, the identity of transition metal in those bimetallic species has a profound impact on the chemoselectivity between allylic amination and olefine aziridination (entries 1–4, Table 1), as the molar ratio of **2** : **3** follows the trend of Co > Cu > Mn ≈ Zn.

Moreover, we have attempted to evaluate how the lattice-confined heterobimetallic sites in the crystalline porous $[(PdM)_3(btc)_4]$ (M = Cu, Zn, Mn, and Co) affect the amination results using compound **1**. Despite 10 mol% MOF loading (calculated based on the $PdM(OOC)_4$ unit), we failed to observe meaningful conversions using $[(PdM)_3(btc)_4]$ (<5%). We attributed this to the small pore size limiting the diffusion of involved reagents including **1** and the large-size $PhI(OAc)_2$ as an oxidant. Therefore, we were motivated to prepare Pd(II)-based heterobimetallic MOFs, which feature a larger accessible pore than that of $[(PdM)_3(btc)_4]$. The mechanochemical synthesis readily enables us to access another family of MOFs, $[(PdM)_3(btb)_4]$ (M = Cu, Zn, Mn, and Co), by replacing H_3btc with 1,3,5-tris(4-carboxyphenyl) benzene (H_3btb), an extended tritopic linker. The resultant crystalline MOFs were confirmed by a suite of solid-state

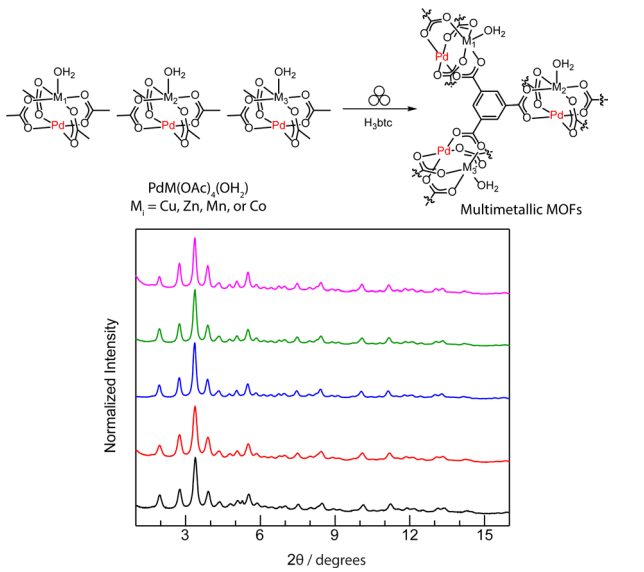

Fig. 5 The developed mechanochemistry affords a family of crystalline multimetallic MOFs ($[(PdCu)_{1.5}(PdZn)_{1.5}(btc)_4]$ (—), $[(PdZn)_{1.5}(PdMn)_{1.5}(btc)_4]$ (—), $[(PdCu)(PdZn)(PdMn)(btc)_4]$ (—), $[(PdCu)_{0.75}(PdZn)_{0.75}(PdMn)_{0.75}(PdCo)_{0.75}(btc)_4]$ (—)), which are isostructural to $[(PdCu)_3(btc)_4]$ (—).The PXRD data were collected or calculated using $\lambda = 0.45212$ Å.

Table 1 Summary of the results from chemoselective amination with molecular catalysts and MOFs.[a] The results demonstrate that the relative order of catalyst selectivity depends on the metal identity

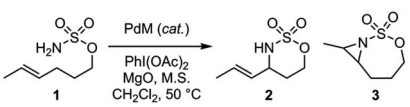

Entry	Catalyst	2 : 3	Yield (%)
1	$PdCo(OAc)_4$	4.4 : 1	85
2	$PdCu(OAc)_4$	1.5 : 1	49
3	$PdMn(OAc)_4$	0.8 : 1	28
4	$PdZn(OAc)_4$	0.7 : 1	29
5	$[(PdCo)_3(btb)_4]$	2.5 : 1	51
6	$[(PdCu)_3(btb)_4]$	1.6 : 1	44
7	$[(PdMn)_3(btb)_4]$	NA	<5
8	$[(PdZn)_3(btb)_4]$	1.1 : 1	13

[a] A 4 mL vial was charged with *trans*-4-hexenyl sulfamate (**1**, 18.0 mg, 0.100 mmol, 1.00 equiv.), $PhI(OAc)_2$ (45.0 mg, 0.140 mmol, 1.40 equiv.), CH_2Cl_2 (600 μL), magnesium oxide (MgO, 12.0 mg), and molecular sieves (M. S., 8.1 mg) with 4.0 mol% molecular heterobimetallic complexes (2.0 mg) or 10 mol% [PdM]-based MOFs (9.4 mg) for 48 h. The reaction mixtures were heated to 50 °C. Product ratios are reported based on integration of gas chromatography (GC) traces (suspension was filtered through a short column containing alumina eluting with EtOAc to remove metal complexes before GC).

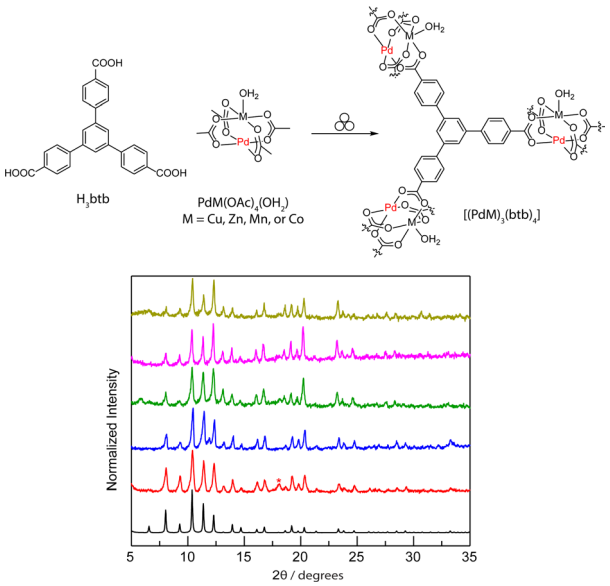

Fig. 6 The developed mechanochemistry affords a family of crystalline large-pore MOFs ([$(PdCu)_3(btb)_4$] (—), [$(PdZn)_3(btb)_4$] (—), [PdCo$(btc)_4$] (—), [$(PdMn)_3(btb)_4$] (—)), which are isostructural to ([$Cu_3(btb)_2$] (calculated (—) and mechanochemically obtained (—)). The PXRD data were collected or calculated using λ = 1.5418 Å. The notable additional peak at 2θ = 18.1° from [$Cu_3(btb)_2$] is tentatively attributed to the unreacted H_3btb ligand residue (see further discussion in Fig. S35†).

characterization techniques including PXRD (Fig. 6), IR (Fig. S29†), TGA (Fig. S30†), and gas adsorption analysis (Fig. S31–S34†).[90] The collected PXRD patterns (Fig. 6) illustrate that these MOFs are isostructural to [$Cu_3(btb)_2$], also known as MOF-14.[53,91]

More importantly, by the employment of these pore-expanded MOFs, we have successfully observed the catalytic conversion of **1** into **2** and **3** (Table 1) and the chemoselectivity of **2** and **3** follows a similar trend observed in the molecular complexes. Given the outlier catalytic performance of [PdCo$(OOC)_4$], we further tested and proved [$(PdCo)_3(btb)_4$] to be an effective heterogeneous catalyst for other substrates, including 3-phenylpropyl sulfamate (Table S8†) and 3-methylbutyl sulfamate (Table S9†) during intramolecular nitrene transfer events. Thus, we highlight that reticular chemistry, commonly encountered in solvothermal reactions, remains effective in the (near) solid state mechanochemical synthesis[78,79] and allows us to access structures with tunable pore space. These large-pore heterobimetallic MOFs exhibit catalytic performances for nitrene transfer reactions, while the current challenge still remains associated with the recyclability of those MOFs. The chemoselectivity for allylic amination *versus* olefin aziridination has been employed as a chemical probe to illustrate that the identity of the first-row metal ion in the Pd(II)-based heterobimetallic cluster affects the reaction outcomes.

Conclusions

In summary, we report a compelling and generalizable mechanochemical synthetic strategy to build versatile Pd(II)-based heterobimetallic MOFs, which features ambient and sustainable reaction conditions and effectively avoids the Pd(II) reduction. This generic and facile strategy provides access to a unique family of Pd(II)-based MOFs. The solid-state mechanochemistry leads to a number of remarkable synthetic advantages that include short reaction time, minimum solvent requirement, high reaction yield, and good control over metal compositions. We also further examined the applications of lattice-confined heterobimetallic sites in large-pore frameworks and proved [$(PdCo)_3(btb)_4$] to be a potential heterogeneous catalyst for nitrene transfer chemistry. We expect the developed mechanochemistry to not only trigger further efforts on investigating the unique delivery of mechanochemistry, but also more explorations on new exciting chemistry of Pd(II)-based MOFs not typically accessible by conventional means.

Data availability

The data (experimental procedures and characterization data) that support this article is available within the article and its ESI.†

Author contributions

WG and ZT conceived and designed the project and wrote the manuscript draft. ZT carried out materials synthesis and characterization as well as performing data analysis. JM, JW, MD, GR, and WX contributed to materials characterization. All authors discussed the results and commented on the manuscript.

Conflicts of interest

There are no conflicts to declare.

Acknowledgements

This work is supported by the National Science Foundation under grant no. 2345469. Exploratory studies of the mechanochemistry were supported by the start-up funds of New Mexico Tech and Ohio University. Synchrotron PXRD data were collected at Beamline 17-BM of Advanced Photon Source (APS), Argonne National Laboratory. XAS data were collected at The Materials Research Collaborative Access Team (MRCAT) at APS, supported by the Department of Energy and the MRCAT member institutions. Use of the APS, an Office of Science User Facility operated for the U.S. Department of Energy (DOE) Office of Science by Argonne National Laboratory, was supported by the U.S. DOE under contract no. DE-AC02-06CH11357.

References

1 H. Furukawa, K. E. Cordova, M. O'Keeffe and O. M. Yaghi, The chemistry and applications of metal-organic frameworks, *Science*, 2013, **341**, 1230444.
2 H. C. Zhou and S. Kitagawa, Metal-organic frameworks (MOFs), *Chem. Soc. Rev.*, 2014, **43**, 5415–5418.

3 S. P. Shet, S. Shanmuga Priya, K. Sudhakar and M. Tahir, A review on current trends in potential use of metal-organic framework for hydrogen storage, *Int. J. Hydrogen Energy*, 2021, **46**, 11782–11803.
4 B. Li, H. M. Wen, W. Zhou and B. Chen, Porous Metal-Organic Frameworks for Gas Storage and Separation: What, How, and Why?, *J. Phys. Chem. Lett.*, 2014, **5**, 3468–3479.
5 X. Zhao, Y. Wang, D.-S. Li, X. Bu and P. Feng, Metal–Organic Frameworks for Separation, *Adv. Mater.*, 2018, **30**, 1705189.
6 R.-B. Lin, S. Xiang, W. Zhou and B. Chen, Microporous Metal-Organic Framework Materials for Gas Separation, *Chem*, 2020, **6**, 337–363.
7 W. Fan, X. Zhang, Z. Kang, X. Liu and D. Sun, Isoreticular chemistry within metal–organic frameworks for gas storage and separation, *Coord. Chem. Rev.*, 2021, **443**, 213968.
8 V. Pascanu, G. Gonzalez Miera, A. K. Inge and B. Martin-Matute, Metal-Organic Frameworks as Catalysts for Organic Synthesis: A Critical Perspective, *J. Am. Chem. Soc.*, 2019, **141**, 7223–7234.
9 Q. Wang and D. Astruc, State of the Art and Prospects in Metal-Organic Framework (MOF)-Based and MOF-Derived Nanocatalysis, *Chem. Rev.*, 2020, **120**, 1438–1511.
10 A. A. Ezazi, W.-Y. Gao and D. C. Powers, Leveraging Exchange Kinetics for the Synthesis of Atomically Precise Porous Catalysts, *ChemCatChem*, 2021, **13**, 2117–2131.
11 A. Dhakshinamoorthy, Z. Li and H. Garcia, Catalysis and photocatalysis by metal organic frameworks, *Chem. Soc. Rev.*, 2018, **47**, 8134–8172.
12 J. R. Bour, A. M. Wright, X. He and M. Dincă, Bioinspired chemistry at MOF secondary building units, *Chem. Sci.*, 2020, **11**, 1728–1737.
13 A. E. Baumann, D. A. Burns, B. Liu and V. S. Thoi, Metal-organic framework functionalization and design strategies for advanced electrochemical energy storage devices, *Commun. Chem.*, 2019, **2**, 86.
14 X. Chen, K. M. Engle, D.-H. Wang and J.-Q. Yu, Palladium(II)-Catalyzed C–H Activation/C–C Cross-Coupling Reactions: Versatility and Practicality, *Angew. Chem., Int. Ed.*, 2009, **48**, 5094–5115.
15 C. C. C. Johansson Seechurn, M. O. Kitching, T. J. Colacot and V. Snieckus, Palladium-Catalyzed Cross-Coupling: A Historical Contextual Perspective to the 2010 Nobel Prize, *Angew. Chem., Int. Ed.*, 2012, **51**, 5062–5085.
16 J. R. Naber and S. L. Buchwald, Palladium-Catalyzed Stille Cross-Coupling Reaction of Aryl Chlorides using a Pre-Milled Palladium Acetate and XPhos Catalyst System, *Adv. Synth. Catal.*, 2008, **350**, 957–961.
17 H. G. Tang and D. C. Sherrington, Polymer-Supported Pd(II) Wacker-Type Catalysts II. Application in the Oxidation of Dec-1-ene, *J. Catal.*, 1993, **142**, 540–551.
18 J. A. Mueller, C. P. Goller and M. S. Sigman, Elucidating the Significance of β-Hydride Elimination and the Dynamic Role of Acid/Base Chemistry in a Palladium-Catalyzed Aerobic Oxidation of Alcohols, *J. Am. Chem. Soc.*, 2004, **126**, 9724–9734.
19 F. X. Llabrés i Xamena, A. Abad, A. Corma and H. Garcia, MOFs as catalysts: Activity, reusability and shape-selectivity of a Pd-containing MOF, *J. Catal.*, 2007, **250**, 294–298.
20 J. A. R. Navarro, E. Barea, J. M. Salas, N. Masciocchi, S. Galli, A. Sironi, C. O. Ania and J. B. Parra, H_2, N_2, CO, and CO_2 Sorption Properties of a Series of Robust Sodalite-Type Microporous Coordination Polymers, *Inorg. Chem.*, 2006, **45**, 2397–2399.
21 M. Perfecto-Irigaray, J. Albo, G. Beobide, O. Castillo, A. Irabien and S. Pérez-Yáñez, Synthesis of heterometallic metal-organic frameworks and their performance as electrocatalyst for CO_2 reduction, *RSC Adv.*, 2018, **8**, 21092–21099.
22 I. Bratsos, C. Tampaxis, I. Spanopoulos, N. Demitri, G. Charalambopoulou, D. Vourloumis, T. A. Steriotis and P. N. Trikalitis, Heterometallic In(III)-Pd(II) Porous Metal-Organic Framework with Square-Octahedron Topology Displaying High CO_2 Uptake and Selectivity toward CH_4 and N_2, *Inorg. Chem.*, 2018, **57**, 7244–7251.
23 E. Miguel-Casañ, M. D. Darawsheh, V. Fariña-Torres, I. J. Vitórica-Yrezábal, E. Andres-Garcia, M. Fañanás-Mastral and G. M. Espallargas, Heterometallic palladium-iron metal-organic framework as a highly active catalyst for cross-coupling reactions, *Chem. Sci.*, 2022, **14**, 179–185.
24 C.-H. Wang, W.-Y. Gao, Q. Ma and D. C. Powers, Templating metastable Pd_2 carboxylate aggregates, *Chem. Sci.*, 2019, **10**, 1823–1830.
25 T. He, X.-J. Kong, J. Zhou, C. Zhao, K. Wang, X.-Q. Wu, X.-L. Lv, G.-R. Si, J.-R. Li and Z.-R. Nie, A Practice of Reticular Chemistry: Construction of a Robust Mesoporous Palladium Metal-Organic Framework via Metal Metathesis, *J. Am. Chem. Soc.*, 2021, **143**, 9901–9911.
26 S. Parshamoni, R. Nasani, A. Paul and S. Konar, Synthesis of a palladium based MOF via an effective post-synthetic modification approach and its catalytic activity towards Heck type coupling reactions, *Inorg. Chem. Front.*, 2021, **8**, 693–699.
27 D. Kim, K. S. Song, O. Buyukcakir, T. Yildirim and A. Coskun, Bimetallic metal organic frameworks with precisely positioned metal centers for efficient H_2 storage, *Chem. Commun.*, 2018, **54**, 12218–12221.
28 J. M. Teo, C. J. Coghlan, J. D. Evans, E. Tsivion, M. Head-Gordon, C. J. Sumby and C. J. Doonan, Hetero-bimetallic metal–organic polyhedra, *Chem. Commun.*, 2016, **52**, 276–279.
29 Solvothermal reaction conditions that were routinely applied to obtain $[Cu_3(btc)_2]$ (a mixture of DMF, H_2O, and EtOH at 85 °C for 24 h) were attempted for the synthesis of $[(PdM)_3(btc)_4]$ (M = Ni or Co) without success, Those solvothermal reactions in the presence of $PdM(OAc)_4$ (M = Ni or Co) lead to the formation of Pd black.
30 S. Głowniak, B. Szczęśniak, J. Choma and M. Jaroniec, Mechanochemistry: Toward green synthesis of metal–organic frameworks, *Mater. Today*, 2021, **46**, 109–124.
31 B. Szczęśniak, S. Borysiuk, J. Choma and M. Jaroniec, Mechanochemical synthesis of highly porous materials, *Mater. Horiz.*, 2020, **7**, 1457–1473.

32 T. Friščić, C. Mottillo and H. M. Titi, Mechanochemistry for Synthesis, *Angew. Chem., Int. Ed.*, 2020, **59**, 1018–1029.
33 D. Chen, J. Zhao, P. Zhang and S. Dai, Mechanochemical synthesis of metal–organic frameworks, *Polyhedron*, 2019, **162**, 59–64.
34 C.-A. Tao and J.-F. Wang, Synthesis of Metal Organic Frameworks by Ball-Milling, *Crystals*, 2020, **11**, 15.
35 T. Stolar and K. Užarević, Mechanochemistry: an efficient and versatile toolbox for synthesis, transformation, and functionalization of porous metal-organic frameworks, *CrystEngComm*, 2020, **22**, 4511–4525.
36 F. Afshariazar and A. Morsali, The unique opportunities of mechanosynthesis in green and scalable fabrication of metal–organic frameworks, *J. Mater. Chem. A*, 2022, **10**, 15332–15369.
37 J.-L. Do and T. Friščić, Mechanochemistry: A Force of Synthesis, *ACS Cent. Sci.*, 2017, **3**, 13–19.
38 G. A. Bowmaker, Solvent-assisted mechanochemistry, *Chem. Commun.*, 2013, **49**, 334–348.
39 S. L. James, C. J. Adams, C. Bolm, D. Braga, P. Collier, T. Friščić, F. Grepioni, K. D. M. Harris, G. Hyett, W. Jones, A. Krebs, J. Mack, L. Maini, A. G. Orpen, I. P. Parkin, W. C. Shearouse, J. W. Steed and D. C. Waddell, Mechanochemistry: opportunities for new and cleaner synthesis, *Chem. Soc. Rev.*, 2012, **41**, 413–447.
40 T. Friščić, New opportunities for materials synthesis using mechanochemistry, *J. Mater. Chem.*, 2010, **20**, 7599–7605.
41 A. Pichon, A. Lazuen-Garay and S. L. James, Solvent-free synthesis of a microporous metal-organic framework, *CrystEngComm*, 2006, **8**, 211–214.
42 W. Yuan, J. O'Connor and S. L. James, Mechanochemical synthesis of homo- and hetero-rare-earth(III) metal–organic frameworks by ball milling, *CrystEngComm*, 2010, **12**, 3515–3517.
43 D. Crawford, J. Casaban, R. Haydon, N. Giri, T. McNally and S. L. James, Synthesis by extrusion: continuous, large-scale preparation of MOFs using little or no solvent, *Chem. Sci.*, 2015, **6**, 1645–1649.
44 W. Yuan, A. L. Garay, A. Pichon, R. Clowes, C. D. Wood, A. I. Cooper and S. L. James, Study of the mechanochemical formation and resulting properties of an archetypal MOF: Cu3(BTC)2 (BTC = 1,3,5-benzenetricarboxylate), *CrystEngComm*, 2010, **12**, 4063–4065.
45 P. A. Julien, K. Užarević, A. D. Katsenis, S. A. J. Kimber, T. Wang, O. K. Farha, Y. Zhang, J. Casaban, L. S. Germann, M. Etter, R. E. Dinnebier, S. L. James, I. Halasz and T. Friščić, *In Situ* Monitoring and Mechanism of the Mechanochemical Formation of a Microporous MOF-74 Framework, *J. Am. Chem. Soc.*, 2016, **138**, 2929–2932.
46 P. J. Beldon, L. Fábián, R. S. Stein, A. Thirumurugan, A. K. Cheetham and T. Friščić, Rapid room-temperature synthesis of zeolitic imidazolate frameworks by using mechanochemistry, *Angew. Chem., Int. Ed.*, 2010, **49**, 9640–9643.
47 T. Friščić and L. Fábián, Mechanochemical conversion of a metal oxide into coordination polymers and porous frameworks using liquid-assisted grinding (LAG), *CrystEngComm*, 2009, **11**, 743–745.
48 Z. Akimbekov, A. D. Katsenis, G. P. Nagabhushana, G. Ayoub, M. Arhangelskis, A. J. Morris, T. Friščić and A. Navrotsky, Experimental and Theoretical Evaluation of the Stability of True MOF Polymorphs Explains Their Mechanochemical Interconversions, *J. Am. Chem. Soc.*, 2017, **139**, 7952–7957.
49 B. Karadeniz, D. Žilić, I. Huskić, L. S. Germann, A. M. Fidelli, S. Muratović, I. Lončarić, M. Etter, R. E. Dinnebier, D. Barišić, N. Cindro, T. Islamoglu, O. K. Farha, T. Friščić and K. Užarević, Controlling the Polymorphism and Topology Transformation in Porphyrinic Zirconium Metal-Organic Frameworks via Mechanochemistry, *J. Am. Chem. Soc.*, 2019, **141**, 19214–19220.
50 G. Ayoub, B. Karadeniz, A. J. Howarth, O. K. Farha, I. Đilović, L. S. Germann, R. E. Dinnebier, K. Užarević and T. Friščić, Rational Synthesis of Mixed-Metal Microporous Metal–Organic Frameworks with Controlled Composition Using Mechanochemistry, *Chem. Mater.*, 2019, **31**, 5494–5501.
51 B. Karadeniz, A. J. Howarth, T. Stolar, T. Islamoglu, I. Dejanović, M. Tireli, M. C. Wasson, S.-Y. Moon, O. K. Farha, T. Friščić and K. Užarević, Benign by Design: Green and Scalable Synthesis of Zirconium UiO-Metal–Organic Frameworks by Water-Assisted Mechanochemistry, *ACS Sustainable Chem. Eng.*, 2018, **6**, 15841–15849.
52 M. Klimakow, P. Klobes, A. F. Thünemann, K. Rademann and F. Emmerling, Mechanochemical Synthesis of Metal−Organic Frameworks: A Fast and Facile Approach toward Quantitative Yields and High Specific Surface Areas, *Chem. Mater.*, 2010, **22**, 5216–5221.
53 M. Klimakow, P. Klobes, K. Rademann and F. Emmerling, Characterization of mechanochemically synthesized MOFs, *Microporous Mesoporous Mater.*, 2012, **154**, 113–118.
54 L. Tröbs, M. Wilke, W. Szczerba, U. Reinholz and F. Emmerling, Mechanochemical synthesis and characterisation of two new bismuth metal organic frameworks, *CrystEngComm*, 2014, **16**, 5560–5565.
55 A.-A. Al-Terkawi, G. Scholz, F. Emmerling and E. Kemnitz, Mechanochemical Synthesis, Characterization, and Structure Determination of New Alkaline Earth Metal-Tetrafluoroterephthalate Frameworks: Ca(pBDC-F4)·4H2O, Sr(pBDC-F4)·4H2O, and Ba(pBDC-F4), *Cryst. Growth Des.*, 2016, **16**, 1923–1933.
56 A.-A. Al-Terkawi, G. Scholz, F. Emmerling and E. Kemnitz, Strontium-coordination polymers based on tetrafluorophthalic and phthalic acids: mechanochemical synthesis, ab initio structures determination, and spectroscopic characterization, *Dalton Trans.*, 2017, **46**, 12574–12587.
57 J. Nawrocki, D. Prochowicz, A. Wiśniewski, I. Justyniak, P. Goś and J. Lewiński, Development of an SBU-Based Mechanochemical Approach for Drug-Loaded MOFs, *Eur. J. Inorg. Chem.*, 2020, **2020**, 796–800.
58 D. Prochowicz, J. Nawrocki, M. Terlecki, W. Marynowski and J. Lewiński, Facile Mechanosynthesis of the Archetypal Zn-Based Metal-Organic Frameworks, *Inorg. Chem.*, 2018, **57**, 13437–13442.

59 D. Prochowicz, K. Sokołowski, I. Justyniak, A. Kornowicz, D. Fairen-Jimenez, T. Friščić and J. Lewiński, A mechanochemical strategy for IRMOF assembly based on pre-designed oxo-zinc precursors, *Chem. Commun.*, 2015, **51**, 4032–4035.

60 I. Brekalo, W. Yuan, C. Mottillo, Y. Lu, Y. Zhang, J. Casaban, K. T. Holman, S. L. James, F. Duarte, P. A. Williams, K. D. M. Harris and T. Friščić, Manometric real-time studies of the mechanochemical synthesis of zeolitic imidazolate frameworks, *Chem. Sci.*, 2020, **11**, 2141–2147.

61 J. R. Ramirez, H. Yang, C. M. Kane, A. N. Ley and K. T. Holman, Reproducible Synthesis and High Porosity of mer-Zn(Im)$_2$ (ZIF-10): Exploitation of an Apparent Double-Eight Ring Template, *J. Am. Chem. Soc.*, 2016, **138**, 12017–12020.

62 I. Brekalo, C. M. Kane, A. N. Ley, J. R. Ramirez, T. Friščić and K. T. Holman, Use of a "Shoe-Last" Solid-State Template in the Mechanochemical Synthesis of High-Porosity RHO-Zinc Imidazolate, *J. Am. Chem. Soc.*, 2018, **140**, 10104–10108.

63 I. Brekalo, D. E. Deliz, C. M. Kane, T. Friščić and K. T. Holman, Exploring the Scope of Macrocyclic "Shoe-last" Templates in the Mechanochemical Synthesis of RHO Topology Zeolitic Imidazolate Frameworks (ZIFs), *Molecules*, 2020, **25**, 633.

64 D. Lv, Y. Chen, Y. Li, R. Shi, H. Wu, X. Sun, J. Xiao, H. Xi, Q. Xia and Z. Li, Efficient Mechanochemical Synthesis of MOF-5 for Linear Alkanes Adsorption, *J. Chem. Eng. Data*, 2017, **62**, 2030–2036.

65 Y. Chen, H. Wu, Z. Liu, X. Sun, Q. Xia and Z. Li, Liquid-Assisted Mechanochemical Synthesis of Copper Based MOF-505 for the Separation of CO_2 over CH_4 or N_2, *Ind. Eng. Chem. Res.*, 2018, **57**, 703–709.

66 Y. Chen, J. Xiao, D. Lv, T. Huang, F. Xu, X. Sun, H. Xi, Q. Xia and Z. Li, Highly efficient mechanochemical synthesis of an indium based metal-organic framework with excellent water stability, *Chem. Eng. Sci.*, 2017, **158**, 539–544.

67 H. K. Lee, J. H. Lee and H. R. Moon, Mechanochemistry as a Reconstruction Tool of Decomposed Metal-Organic Frameworks, *Inorg. Chem.*, 2021, **60**, 11825–11829.

68 E. Y. Chen, R. M. Mandel and P. J. Milner, Evaluating solvothermal and mechanochemical routes towards the metal–organic framework Mg_2(m-dobdc), *CrystEngComm*, 2022, **24**, 7292–7297.

69 Z. Wang, Z. Li, M. Ng and P. J. Milner, Rapid mechanochemical synthesis of metal–organic frameworks using exogenous organic base, *Dalton Trans.*, 2020, **49**, 16238–16244.

70 Y. Shi, B. Liang, A. Alsalme, R.-B. Lin and B. Chen, Mechanochemical synthesis of an ethylene sieve UTSA-280, *J. Solid State Chem.*, 2020, **287**, 121321.

71 M. F. Thorne, M. L. R. Gomez, A. M. Bumstead, S. Li and T. D. Bennett, Mechanochemical synthesis of mixed metal, mixed linker, glass-forming metal-organic frameworks, *Green Chem.*, 2020, **22**, 2505–2512.

72 O. Barreda, G. R. Lorzing and E. D. Bloch, Mechanochemical synthesis of two-dimensional metal-organic frameworks, *Powder Diffr.*, 2019, **34**, 119–123.

73 S. Darwish, S.-Q. Wang, D. M. Croker, G. M. Walker and M. J. Zaworotko, Comparison of Mechanochemistry vs Solution Methods for Synthesis of 4,4′-Bipyridine-Based Coordination Polymers, *ACS Sustainable Chem. Eng.*, 2019, **7**, 19505–19512.

74 F. E. Salvador, V. Miller, K. Shimada, C.-H. Wang, J. Wright, M. Das, Y.-P. Chen, Y.-S. Chen, C. Sheehan, W. Xu, G. Rubasinghege and W.-Y. Gao, Mechanochemistry of Group 4 Element-Based Metal–Organic Frameworks, *Inorg. Chem.*, 2021, **60**, 16079–16084.

75 K. Užarević, T. C. Wang, S.-Y. Moon, A. M. Fidelli, J. T. Hupp, O. K. Farha and T. Friščić, Mechanochemical and solvent-free assembly of zirconium-based metal-organic frameworks, *Chem. Commun.*, 2016, **52**, 2133–2136.

76 T. Stolar, L. Batzdorf, S. Lukin, D. Žilić, C. Motillo, T. Friščić, F. Emmerling, I. Halasz and K. Užarević, Situ Monitoring of the Mechanosynthesis of the Archetypal Metal-Organic Framework HKUST-1: Effect of Liquid Additives on the Milling Reactivity, *Inorg. Chem.*, 2017, **56**, 6599–6608.

77 F. E. Salvador, J. O. Barajas and W.-Y. Gao Mechanochemical, Access to Catechol-Derived Metal-Organic Frameworks, *Inorg. Chem.*, 2023, **62**, 3333–3337.

78 W.-Y. Gao, A. Sur, C.-H. Wang, G. R. Lorzing, A. M. Antonio, G. A. Taggart, A. A. Ezazi, N. Bhuvanesh, E. D. Bloch and D. C. Powers, Atomically Precise Crystalline Materials Based on Kinetically Inert Metal Ions via Reticular Mechanopolymerization, *Angew. Chem., Int. Ed.*, 2020, **59**, 10878–10883.

79 A. M. Fidelli, B. Karadeniz, A. J. Howarth, I. Huskić, L. S. Germann, I. Halasz, M. Etter, S.-Y. Moon, R. E. Dinnebier, V. Stilinović, O. K. Farha, T. Friščić and K. Užarević, Green and rapid mechanosynthesis of high-porosity NU- and UiO-type metal-organic frameworks, *Chem. Commun.*, 2018, **54**, 6999–7002.

80 N. S. Akhmadullina, N. V. Cherkashina, N. Y. Kozitsyna, I. P. Stolarov, E. V. Perova, A. E. Gekhman, S. E. Nefedov, M. N. Vargaftik and I. I. Moiseev, Synthesis of palladium(II) 3d-metal(II) paddlewheel acetate-bridged heterodimetallic complexes: Unexpected catalysis by water molecules, *Inorg. Chim. Acta*, 2009, **362**, 1943–1951.

81 S. S.-Y. Chui, S. M.-F. Lo, J. P. H. Charmant, A. G. Orpen and I. D. Williams, A Chemically Functionalizable Nanoporous Material $[Cu_3(TMA)_2(H_2O)_3]_n$, *Science*, 1999, **283**, 1148–1150.

82 C. R. Wade and M. Dincă, Investigation of the synthesis, activation, and isosteric heats of CO_2 adsorption of the isostructural series of metal–organic frameworks $M_3(BTC)_2$ (M = Cr, Fe, Ni, Cu, Mo, Ru), *Dalton Trans.*, 2012, **41**, 7931–7938.

83 A. C. Skapski and M. L. Smart, The crystal structure of trimeric palladium(II) acetate, *J. Chem. Soc., Chem. Commun.*, 1970, 658–659.

84 V. I. Bakhmutov, J. F. Berry, F. A. Cotton, S. Ibragimov and C. A. Murillo, Non-trivial behavior of palladium(ii) acetate, *Dalton Trans.*, 2005, 1989–1992.

85 The incomplete disappearance of the carbonyl C=O stretch around 1720 cm^{-1} and the C–O stretch at 1273 cm^{-1} from free carboxylic acid is likely caused by some defects

encountered in the solid-state synthesis. This also reflects in the small hysteresis loop observed in the N_2 adsorption–desorption isotherms at 77 K (Fig. 3b).

86 L. Helm and A. E. Merbach, Water exchange on metal ions: experiments and simulations, *Coord. Chem. Rev.*, 1999, **187**, 151–181.

87 F. E. Salvador, Z. Tegudeer, H. Locke and W.-Y. Gao, Facile mechanochemical synthesis of MIL-53 and its isoreticular analogues with a glance at reaction reversibility, *Dalton Trans.*, 2024, **53**, 4406–4411.

88 P.-H. Ho, C.-C. Hung, Y.-H. Wang and G. J. Chuang, Intermolecular Nitrene Insertion by Bimetallic Catalysts, *Asian J. Org. Chem.*, 2019, **8**, 275–278.

89 G. H. Huang, J. M. Li, J. J. Huang, J. D. Lin and G. J. Chuang, Cooperative Effect of Two Metals: $CoPd(OAc)_4$-Catalyzed C–H Amination and Aziridination, *Chem.–Eur. J.*, 2014, **20**, 5240–5243.

90 Relatively low values of N_2 uptake observed in the cases of $[(PdCo)_3(btb)_4]$ (Fig. S32†), $[(PdMn)_3(btb)_4]$ (Fig. S33†), and $[(PdZn)_3(btb)_4]$ (Fig. S34†) are likely caused by unreacted H_3btb potentially trapped in cavities, consistent with minor PXRD (Fig. 6) diffraction and IR (Fig. S29†) peaks in these samples. The presence of trapped, unreacted H_3btb is unsurprising, as reactants in the solid phase typically exhibit lower reversibility and mobility compared to those in solution. The known BET surface area values for MOF-14 range from 628 m^2/g to 1215 m^2/g. In comparison, our BET surface areas (P/P_0 = 0.02–0.15) are 1286 m^2/g for $[(PdCu)_3(btb)_4]$, 909 m^2/g for $[(PdCo)_3(btb)_4]$, 581 m^2/g for $[(PdMn)_3(btb)_4]$, and 765 m^2/g for $[(PdZn)_3(btb)_4]$.

91 B. Chen, M. Eddaoudi, S. T. Hyde, M. O'Keeffe and O. M. Yaghi, Interwoven Metal-Organic Framework on a Periodic Minimal Surface with Extra-Large Pores, *Science*, 2001, **291**, 1021–1023.